PHYSICAL REVIEW D **80,** 071102(R) (2009)

Combination of $t\bar{t}$ cross section measurements and constraints on the mass of the top quark and its decays into charged Higgs bosons

V. M. Abazov,[37] B. Abbott,[75] M. Abolins,[65] B. S. Acharya,[30] M. Adams,[51] T. Adams,[49] E. Aguilo,[6] M. Ahsan,[59] G. D. Alexeev,[37] G. Alkhazov,[41] A. Alton,[64,*] G. Alverson,[63] G. A. Alves,[2] L. S. Ancu,[36] T. Andeen,[53] M. S. Anzelc,[53] M. Aoki,[50] Y. Arnoud,[14] M. Arov,[60] M. Arthaud,[18] A. Askew,[49,†] B. Åsman,[42] O. Atramentov,[49,†] C. Avila,[8] J. BackusMayes,[82] F. Badaud,[13] L. Bagby,[50] B. Baldin,[50] D. V. Bandurin,[59] S. Banerjee,[30] E. Barberis,[63] A.-F. Barfuss,[15] P. Bargassa,[80] P. Baringer,[58] J. Barreto,[2] J. F. Bartlett,[50] U. Bassler,[18] D. Bauer,[44] S. Beale,[6] A. Bean,[58] M. Begalli,[3] M. Begel,[73] C. Belanger-Champagne,[42] L. Bellantoni,[50] A. Bellavance,[50] J. A. Benitez,[65] S. B. Beri,[28] G. Bernardi,[17] R. Bernhard,[23] I. Bertram,[43] M. Besançon,[18] R. Beuselinck,[44] V. A. Bezzubov,[40] P. C. Bhat,[50] V. Bhatnagar,[28] G. Blazey,[52] S. Blessing,[49] K. Bloom,[67] A. Boehnlein,[50] D. Boline,[62] T. A. Bolton,[59] E. E. Boos,[39] G. Borissov,[43] T. Bose,[62] A. Brandt,[78] R. Brock,[65] G. Brooijmans,[70] A. Bross,[50] D. Brown,[19] X. B. Bu,[7] D. Buchholz,[53] M. Buehler,[81] V. Buescher,[22] V. Bunichev,[39] S. Burdin,[43,‡] T. H. Burnett,[82] C. P. Buszello,[44] P. Calfayan,[26] B. Calpas,[15] S. Calvet,[16] J. Cammin,[71] M. A. Carrasco-Lizarraga,[34] E. Carrera,[49] W. Carvalho,[3] B. C. K. Casey,[50] H. Castilla-Valdez,[34] S. Chakrabarti,[72] D. Chakraborty,[52] K. M. Chan,[55] A. Chandra,[48] E. Cheu,[46] S. Chevalier-Théry,[18] D. K. Cho,[62] S. Choi,[33] B. Choudhary,[29] T. Christoudias,[44] S. Cihangir,[50] D. Claes,[67] J. Clutter,[58] M. Cooke,[50] W. E. Cooper,[50] M. Corcoran,[80] F. Couderc,[18] M.-C. Cousinou,[15] S. Crépé-Renaudin,[14] V. Cuplov,[59] D. Cutts,[77] M. Ćwiok,[31] A. Das,[46] G. Davies,[44] K. De,[78] S. J. de Jong,[36] E. De La Cruz-Burelo,[34] K. DeVaughan,[67] F. Déliot,[18] M. Demarteau,[50] R. Demina,[71] D. Denisov,[50] S. P. Denisov,[40] S. Desai,[50] H. T. Diehl,[50] M. Diesburg,[50] A. Dominguez,[67] T. Dorland,[82] A. Dubey,[29] L. V. Dudko,[39] L. Duflot,[16] D. Duggan,[49] A. Duperrin,[15] S. Dutt,[28] A. Dyshkant,[52] M. Eads,[67] D. Edmunds,[65] J. Ellison,[48] V. D. Elvira,[50] Y. Enari,[77] S. Eno,[61] P. Ermolov,[39,‡‡] M. Escalier,[15] H. Evans,[54] A. Evdokimov,[73] V. N. Evdokimov,[40] G. Facini,[63] A. V. Ferapontov,[59] T. Ferbel,[61,71] F. Fiedler,[25] F. Filthaut,[36] W. Fisher,[50] H. E. Fisk,[50] M. Fortner,[52] H. Fox,[43] S. Fu,[50] S. Fuess,[50] T. Gadfort,[70] C. F. Galea,[36] A. Garcia-Bellido,[71] V. Gavrilov,[38] P. Gay,[13] W. Geist,[19] W. Geng,[15,65] C. E. Gerber,[51] Y. Gershtein,[49,†] D. Gillberg,[6] G. Ginther,[50,71] B. Gómez,[8] A. Goussiou,[82] P. D. Grannis,[72] S. Greder,[19] H. Greenlee,[50] Z. D. Greenwood,[60] E. M. Gregores,[4] G. Grenier,[20] Ph. Gris,[13] J.-F. Grivaz,[16] A. Grohsjean,[26] S. Grünendahl,[50] M. W. Grünewald,[31] F. Guo,[72] J. Guo,[72] G. Gutierrez,[50] P. Gutierrez,[75] A. Haas,[70] N. J. Hadley,[61] P. Haefner,[26] S. Hagopian,[49] J. Haley,[68] I. Hall,[65] R. E. Hall,[47] L. Han,[7] K. Harder,[45] A. Harel,[71] J. M. Hauptman,[57] J. Hays,[44] T. Hebbeker,[21] D. Hedin,[52] J. G. Hegeman,[35] A. P. Heinson,[48] U. Heintz,[62] C. Hensel,[24] I. Heredia-De La Cruz,[34] K. Herner,[64] G. Hesketh,[63] M. D. Hildreth,[55] R. Hirosky,[81] T. Hoang,[49] J. D. Hobbs,[72] B. Hoeneisen,[12] M. Hohlfeld,[22] S. Hossain,[75] P. Houben,[35] Y. Hu,[72] Z. Hubacek,[10] N. Huske,[17] V. Hynek,[10] I. Iashvili,[69] R. Illingworth,[50] A. S. Ito,[50] S. Jabeen,[62] M. Jaffré,[16] S. Jain,[75] K. Jakobs,[23] D. Jamin,[15] C. Jarvis,[61] R. Jesik,[44] K. Johns,[46] C. Johnson,[70] M. Johnson,[50] D. Johnston,[67] A. Jonckheere,[50] P. Jonsson,[44] A. Juste,[50] E. Kajfasz,[15] D. Karmanov,[39] P. A. Kasper,[50] I. Katsanos,[67] V. Kaushik,[78] R. Kehoe,[79] S. Kermiche,[15] N. Khalatyan,[50] A. Khanov,[76] A. Kharchilava,[69] Y. N. Kharzheev,[37] D. Khatidze,[70] T. J. Kim,[32] M. H. Kirby,[53] M. Kirsch,[21] B. Klima,[50] J. M. Kohli,[28] J.-P. Konrath,[23] A. V. Kozelov,[40] J. Kraus,[65] T. Kuhl,[25] A. Kumar,[69] A. Kupco,[11] T. Kurča,[20] V. A. Kuzmin,[39] J. Kvita,[9] F. Lacroix,[13] D. Lam,[55] S. Lammers,[54] G. Landsberg,[77] P. Lebrun,[20] W. M. Lee,[50] A. Leflat,[39] J. Lellouch,[17] J. Li,[78,‡‡] L. Li,[48] Q. Z. Li,[50] S. M. Lietti,[5] J. K. Lim,[32] D. Lincoln,[50] J. Linnemann,[65] V. V. Lipaev,[40] R. Lipton,[50] Y. Liu,[7] Z. Liu,[6] A. Lobodenko,[41] M. Lokajicek,[11] P. Love,[43] H. J. Lubatti,[82] R. Luna-Garcia,[34,§] A. L. Lyon,[50] A. K. A. Maciel,[2] D. Mackin,[80] P. Mättig,[27] A. Magerkurth,[64] P. K. Mal,[82] H. B. Malbouisson,[3] S. Malik,[67] V. L. Malyshev,[37] Y. Maravin,[59] B. Martin,[14] R. McCarthy,[72] C. L. McGivern,[58] M. M. Meijer,[36] A. Melnitchouk,[66] L. Mendoza,[8] D. Menezes,[52] P. G. Mercadante,[5] M. Merkin,[39] K. W. Merritt,[50] A. Meyer,[21] J. Meyer,[24] J. Mitrevski,[70] R. K. Mommsen,[45] N. K. Mondal,[30] R. W. Moore,[6] T. Moulik,[58] G. S. Muanza,[15] M. Mulhearn,[70] O. Mundal,[22] L. Mundim,[3] E. Nagy,[15] M. Naimuddin,[50] M. Narain,[77] H. A. Neal,[64] J. P. Negret,[8] P. Neustroev,[41] H. Nilsen,[23] H. Nogima,[3] S. F. Novaes,[5] T. Nunnemann,[26] G. Obrant,[41] C. Ochando,[16] D. Onoprienko,[59] J. Orduna,[34] N. Oshima,[50] N. Osman,[44] J. Osta,[55] R. Otec,[10] G. J. Otero y Garzón,[1] M. Owen,[45] M. Padilla,[48] P. Padley,[80] M. Pangilinan,[77] N. Parashar,[56] S.-J. Park,[24] S. K. Park,[32] J. Parsons,[70] R. Partridge,[77] N. Parua,[54] A. Patwa,[73] G. Pawloski,[80] B. Penning,[23] M. Perfilov,[39] K. Peters,[45] Y. Peters,[45] P. Pétroff,[16] R. Piegaia,[1] J. Piper,[65] M.-A. Pleier,[22] P. L. M. Podesta-Lerma,[34,‖] V. M. Podstavkov,[50] Y. Pogorelov,[55] M.-E. Pol,[2] P. Polozov,[38] A. V. Popov,[40] C. Potter,[6] W. L. Prado da Silva,[3] S. Protopopescu,[73] J. Qian,[64] A. Quadt,[24] B. Quinn,[66] A. Rakitine,[43] M. S. Rangel,[16] K. Ranjan,[29] P. N. Ratoff,[43] P. Renkel,[79] P. Rich,[45] M. Rijssenbeek,[72] I. Ripp-Baudot,[19] F. Rizatdinova,[76] S. Robinson,[44] R. F. Rodrigues,[3] M. Rominsky,[75] C. Royon,[18] P. Rubinov,[50] R. Ruchti,[55] G. Safronov,[38] G. Sajot,[14] A. Sánchez-Hernández,[34] M. P. Sanders,[17] B. Sanghi,[50] G. Savage,[50] L. Sawyer,[60] T. Scanlon,[44] D. Schaile,[26]

R. D. Schamberger,[72] Y. Scheglov,[41] H. Schellman,[53] T. Schliephake,[27] S. Schlobohm,[82] C. Schwanenberger,[45] R. Schwienhorst,[65] J. Sekaric,[49] H. Severini,[75] E. Shabalina,[24] M. Shamim,[59] V. Shary,[18] A. A. Shchukin,[40] R. K. Shivpuri,[29] V. Siccardi,[19] V. Simak,[10] V. Sirotenko,[50] P. Skubic,[75] P. Slattery,[71] D. Smirnov,[55] G. R. Snow,[67] J. Snow,[74] S. Snyder,[73] S. Söldner-Rembold,[45] L. Sonnenschein,[21] A. Sopczak,[43] M. Sosebee,[78] K. Soustruznik,[9] B. Spurlock,[78] J. Stark,[14] V. Stolin,[38] D. A. Stoyanova,[40] J. Strandberg,[64] S. Strandberg,[42] M. A. Strang,[69] E. Strauss,[72] M. Strauss,[75] R. Ströhmer,[26] D. Strom,[53] L. Stutte,[50] S. Sumowidagdo,[49] P. Svoisky,[36] M. Takahashi,[45] A. Tanasijczuk,[1] W. Taylor,[6] B. Tiller,[26] F. Tissandier,[13] M. Titov,[18] V. V. Tokmenin,[37] I. Torchiani,[23] D. Tsybychev,[72] B. Tuchming,[18] C. Tully,[68] P. M. Tuts,[70] R. Unalan,[65] L. Uvarov,[41] S. Uvarov,[41] S. Uzunyan,[52] B. Vachon,[6] P. J. van den Berg,[35] R. Van Kooten,[54] W. M. van Leeuwen,[35] N. Varelas,[51] E. W. Varnes,[46] I. A. Vasilyev,[40] P. Verdier,[20] L. S. Vertogradov,[37] M. Verzocchi,[50] D. Vilanova,[18] P. Vint,[44] P. Vokac,[10] M. Voutilainen,[67,¶] R. Wagner,[68] H. D. Wahl,[49] M. H. L. S. Wang,[71] J. Warchol,[55] G. Watts,[82] M. Wayne,[55] G. Weber,[25] M. Weber,[50,**] L. Welty-Rieger,[54] A. Wenger,[23,††] M. Wetstein,[61] A. White,[78] D. Wicke,[25] M. R. J. Williams,[43] G. W. Wilson,[58] S. J. Wimpenny,[48] M. Wobisch,[60] D. R. Wood,[63] T. R. Wyatt,[45] Y. Xie,[77] C. Xu,[64] S. Yacoob,[53] R. Yamada,[50] W.-C. Yang,[45] T. Yasuda,[50] Y. A. Yatsunenko,[37] Z. Ye,[50] H. Yin,[7] K. Yip,[73] H. D. Yoo,[77] S. W. Youn,[53] J. Yu,[78] C. Zeitnitz,[27] S. Zelitch,[81] T. Zhao,[82] B. Zhou,[64] J. Zhu,[72] M. Zielinski,[71] D. Zieminska,[54] L. Zivkovic,[70] V. Zutshi,[52] and E. G. Zverev[39]

(The D0 Collaboration)

[1]*Universidad de Buenos Aires, Buenos Aires, Argentina*
[2]*LAFEX, Centro Brasileiro de Pesquisas Físicas, Rio de Janeiro, Brazil*
[3]*Universidade do Estado do Rio de Janeiro, Rio de Janeiro, Brazil*
[4]*Universidade Federal do ABC, Santo André, Brazil*
[5]*Instituto de Física Teórica, Universidade Estadual Paulista, São Paulo, Brazil*
[6]*University of Alberta, Edmonton, Alberta, Canada; Simon Fraser University, Burnaby, British Columbia, Canada; York University, Toronto, Ontario, Canada; and McGill University, Montreal, Quebec, Canada*
[7]*University of Science and Technology of China, Hefei, People's Republic of China*
[8]*Universidad de los Andes, Bogotá, Colombia*
[9]*Center for Particle Physics, Charles University, Faculty of Mathematics and Physics, Prague, Czech Republic*
[10]*Czech Technical University in Prague, Prague, Czech Republic*
[11]*Center for Particle Physics, Institute of Physics, Academy of Sciences of the Czech Republic, Prague, Czech Republic*
[12]*Universidad San Francisco de Quito, Quito, Ecuador*
[13]*LPC, Université Blaise Pascal, CNRS/IN2P3, Clermont, France*
[14]*LPSC, , USAUniversité Joseph Fourier Grenoble 1, CNRS/IN2P3, Institut National Polytechnique de Grenoble, Grenoble, France*
[15]*CPPM, Aix-Marseille Université, CNRS/IN2P3, Marseille, France*
[16]*LAL, , USAUniversité Paris-Sud, IN2P3/CNRS, Orsay, France*
[17]*LPNHE, IN2P3/CNRS, , USAUniversités Paris VI and VII, Paris, France*
[18]*CEA, Irfu, SPP, Saclay, France*
[19]*IPHC, Université de Strasbourg, CNRS/IN2P3, Strasbourg, France*
[20]*IPNL, Université Lyon 1, CNRS/IN2P3, Villeurbanne, France and Université de Lyon, Lyon, France*
[21]*III. Physikalisches Institut A, RWTH Aachen University, Aachen, Germany*
[22]*Physikalisches Institut, Universität Bonn, Bonn, Germany*
[23]*Physikalisches Institut, Universität Freiburg, Freiburg, Germany*
[24]*II. Physikalisches Institut, Georg-August-Universität G Göttingen, Germany*
[25]*Institut für Physik, Universität Mainz, Mainz, Germany*
[26]*Ludwig-Maximilians-Universität München, München, Germany*
[27]*Fachbereich Physik, University of Wuppertal, Wuppertal, Germany*
[28]*Panjab University, Chandigarh, India*
[29]*Delhi University, Delhi, India*
[30]*Tata Institute of Fundamental Research, Mumbai, India*
[31]*University College Dublin, Dublin, Ireland*
[32]*Korea Detector Laboratory, Korea University, Seoul, Korea*
[33]*SungKyunKwan University, Suwon, Korea*
[34]*CINVESTAV, Mexico City, Mexico*
[35]*FOM-Institute NIKHEF and University of Amsterdam/NIKHEF, Amsterdam, The Netherlands*
[36]*Radboud University Nijmegen/NIKHEF, Nijmegen, The Netherlands*
[37]*Joint Institute for Nuclear Research, Dubna, Russia*
[38]*Institute for Theoretical and Experimental Physics, Moscow, Russia*

[39]*Moscow State University, Moscow, Russia*
[40]*Institute for High Energy Physics, Protvino, Russia*
[41]*Petersburg Nuclear Physics Institute, St. Petersburg, Russia*
[42]*Stockholm University, Stockholm, Sweden, and Uppsala University, Uppsala, Sweden*
[43]*Lancaster University, Lancaster, United Kingdom*
[44]*Imperial College, London, United Kingdom*
[45]*University of Manchester, Manchester, United Kingdom*
[46]*University of Arizona, Tucson, Arizona 85721, USA*
[47]*California State University, Fresno, California 93740, USA*
[48]*University of California, Riverside, California 92521, USA*
[49]*Florida State University, Tallahassee, Florida 32306, USA*
[50]*Fermi National Accelerator Laboratory, Batavia, Illinois 60510, USA*
[51]*University of Illinois at Chicago, Chicago, Illinois 60607, USA*
[52]*Northern Illinois University, DeKalb, Illinois 60115, USA*
[53]*Northwestern University, Evanston, Illinois 60208, USA*
[54]*Indiana University, Bloomington, Indiana 47405, USA*
[55]*University of Notre Dame, Notre Dame, Indiana 46556, USA*
[56]*Purdue University Calumet, Hammond, Indiana 46323, USA*
[57]*Iowa State University, Ames, Iowa 50011, USA*
[58]*University of Kansas, Lawrence, Kansas 66045, USA*
[59]*Kansas State University, Manhattan, Kansas 66506, USA*
[60]*Louisiana Tech University, Ruston, Louisiana 71272, USA*
[61]*University of Maryland, College Park, Maryland 20742, USA*
[62]*Boston University, Boston, Massachusetts 02215, USA*
[63]*Northeastern University, Boston, Massachusetts 02115, USA*
[64]*University of Michigan, Ann Arbor, Michigan 48109, USA*
[65]*Michigan State University, East Lansing, Michigan 48824, USA*
[66]*University of Mississippi, University, Mississippi 38677, USA*
[67]*University of Nebraska, Lincoln, Nebraska 68588, USA*
[68]*Princeton University, Princeton, New Jersey 08544, USA*
[69]*State University of New York, Buffalo, New York 14260, USA*
[70]*Columbia University, New York, New York 10027, USA*
[71]*University of Rochester, Rochester, New York 14627, USA*
[72]*State University of New York, Stony Brook, New York 11794, USA*
[73]*Brookhaven National Laboratory, Upton, New York 11973, USA*
[74]*Langston University, Langston, Oklahoma 73050, USA*
[75]*University of Oklahoma, Norman, Oklahoma 73019, USA*
[76]*Oklahoma State University, Stillwater, Oklahoma 74078, USA*
[77]*Brown University, Providence, Rhode Island 02912, USA*
[78]*University of Texas, Arlington, Texas 76019, USA*
[79]*Southern Methodist University, Dallas, Texas 75275, USA*
[80]*Rice University, Houston, Texas 77005, USA*
[81]*University of Virginia, Charlottesville, Virginia 22901, USA*
[82]*University of Washington, Seattle, Washington 98195, USA*

(Received 31 March 2009; published 19 October 2009)

We combine measurements of the top quark pair production cross section in $p\bar{p}$ collisions in the ℓ + jets, $\ell\ell$, and $\tau\ell$ final states (where ℓ is an electron or muon) at a center of mass energy of $\sqrt{s} = 1.96$ TeV in 1 fb^{-1} of data collected with the D0 detector. For a top quark mass of 170 GeV/c^2, we obtain $\sigma_{t\bar{t}} = 8.18^{+0.98}_{-0.87}$ pb in agreement with the theoretical prediction. Based on predictions from higher order quantum chromodynamics, we extract a mass for the top quark from the combined $t\bar{t}$ cross section, consistent with the world average of the top quark mass. In addition, the ratios of $t\bar{t}$ cross sections in different final states are used to set upper limits on the branching fractions $B(t \to H^+ b \to \tau^+ \nu b)$ and

[*]Visitor from Augustana College, Sioux Falls, SD, USA.
[†]Visitor from Rutgers University, Piscataway, NJ, USA.
[‡]Visitor from The University of Liverpool, Liverpool, United Kingdom.
[§]Visitor from Centro de Investigacion en Computacion-IPN, Mexico City, Mexico.
[‖]Visitor from ECFM, Universidad Autonoma de Sinaloa, Culiacán, Mexico.
[¶]Visitor from Helsinki Institute of Physics, Helsinki, Finland.
[**]Visitor from Universität Bern, Bern, Switzerland.
[††]Visitor from Universität Zürich, Zürich, Switzerland.
[‡‡]Deceased.

$B(t \to H^+ b \to c\bar{s}b)$ as a function of the charged Higgs boson mass.

DOI: 10.1103/PhysRevD.80.071102 PACS numbers: 14.65.Ha, 13.85.Lg, 13.85.Qk, 13.85.Rm

Precise measurements of the production and decay properties of the heaviest known fermion, the top quark, provide important tests of the standard model (SM) and offer a window for searches for new physics. In this paper we measure the top-antitop quark pair ($t\bar{t}$) production cross section and compare it with the SM prediction, extract the top quark pole mass from this measurement, and search for new physics in top quark decays analyzing ratios of the $t\bar{t}$ cross sections measured in different decay channels.

The inclusive $t\bar{t}$ production cross section ($\sigma_{t\bar{t}}$) is measured in different $t\bar{t}$ decay channels assuming SM branching fractions. The comparison of the results to predictions in next-to-leading order perturbative quantum chromodynamics (QCD), including higher order soft-gluon resummations [1–4], yields a direct test of the SM. Ratios of $\sigma_{t\bar{t}}$ measured in different final states are particularly sensitive to non-SM particles that may appear in top quark decays, especially if the boson in the decay is not a SM W boson. An example is the decay into a charged Higgs boson ($t \to H^+ b$), which, as predicted in some models [5], can compete with the SM decay $t \to W^+ b$. Additionally, many experimental uncertainties cancel in the ratios. Furthermore, since $\sigma_{t\bar{t}}$ depends on the mass of the top quark (m_t), it can be used to extract m_t. Such a measurement is less accurate than direct mass measurements, but provides complementary information with different experimental and theoretical uncertainties.

Within the SM, each quark of the $t\bar{t}$ pair is expected to decay nearly 100% of the times into a W boson and a b quark [6]. W bosons can decay hadronically into $q\bar{q}'$ pairs or leptonically into $e\nu_e$, $\mu\nu_\mu$, and $\tau\nu_\tau$ with the τ in turn decaying into an electron, a muon, or hadrons, and associated neutrinos. If one of the W bosons decays hadronically while the other one produces a direct electron or muon or a secondary electron or muon from τ decay, the final state is referred to as the ℓ + jets (or ℓj) channel. If both W bosons decay leptonically, this leads to a dilepton final state containing a pair of electrons, a pair of muons, or an electron and a muon (the $\ell\ell$ channel), or a hadronically decaying tau accompanied either by an electron or a muon (the $\tau\ell$ channel).

Measurements of the individual $t\bar{t}$ cross sections in $\ell\ell$ and $\tau\ell$ channels using about 1 fb^{-1} of $p\bar{p}$ data from the D0 detector at the Fermilab Tevatron collider at $\sqrt{s} =$ 1.96 TeV are available in Ref. [7]. In the ℓ + jets channel, we use the same selection and background estimation as in Ref. [8], but a slightly larger data set and a unified treatment of systematic uncertainties with the $\ell\ell$ and $\tau\ell$ channels. We provide a brief summary of the event selection and analysis procedures below.

In each final state we select data samples enriched in $t\bar{t}$ events by requiring one or two isolated high transverse momentum (p_T) leptons for the ℓ + jets or $\ell\ell$ channel, respectively. At least two high p_T jets are required for $\ell\ell$ and $\tau\ell$ events, and at least three for ℓ + jets events. Further, in all but the $e\mu$ channel, large transverse missing energy ($\not\!\!E_T$) is required to account for the large transverse momenta of neutrinos from W boson or τ lepton decays. In the $e\mu$ final state, a requirement on the sum of the p_T of the highest p_T (leading) lepton and the two leading jets is imposed instead. In the $\mu\mu$ channel, the $\not\!\!E_T$ requirement is supplemented with a requirement on the significance of the $\not\!\!E_T$ measurement, estimated from the p_T of muons and jets, and their expected resolutions. Additional criteria are applied on the invariant mass of the two opposite charge leptons of the same flavor in the ee and $\mu\mu$ channels to reduce the dominant background from $Z/\gamma^* \to \ell^+\ell^-$ events. In the ℓ + jets and $\tau\ell$ channels we require a minimum azimuthal angle separation between the $\not\!\!E_T$ vector and the lepton p_T, $\Delta\phi(\ell, \not\!\!E_T)$, to reduce background from multijet events, where jets are misidentified as electron, muon, or τ. Details of lepton, jet, and $\not\!\!E_T$ identification are provided in Refs. [9,10]. The final selection in these channels demands at least one identified b jet via a neural-network based algorithm [11]. In the ℓ + jets channel we separate events with one or $\geq 2b$-tagged jets due to their different signal over background ratio and systematic uncertainties.

To simplify the combination and extraction of cross section ratios, all channels are constructed to be mutually exclusive. In particular, events with two identified leptons are excluded from the ℓ + jets selection, and all $\tau\ell$ candidates are removed from the rest of the channels.

The compositions of the samples in the ℓ + jets, $\ell\ell$, and $\tau\ell$ channels are shown in Table I. W + jets production dominates the background for the ℓ + jets events, while multijet production is the most important background in the $\tau\ell$ channel. Background in the $\ell\ell$ channels comes mainly from Z + jets production. In the $\ell\ell$ channel, contributions from W + jets production are part of the multijet background. The smaller contribution from diboson production is included in the category labeled ''other background.'' This category also includes the contribution from single top quark production in the ℓ + jets and $\tau\ell$ channels. The signal, W + jets and Z + jets backgrounds are simulated using ALPGEN [12] for the matrix element calculation and PYTHIA [13] for parton showering and hadronization. Diboson and single top backgrounds are simulated with the PYTHIA and SINGLETOP [14] generators, respectively. We estimate the multijet background from the control data samples. The difference in the ratio of $t\bar{t}$ and W + jets events in the e + jets and μ + jets final states is the result of the larger efficiency and misidentified lepton rate in the e + jets channel compensating for the lower

TABLE I. Expected numbers of background and signal events for $\sigma_{t\bar{t}} = 8.18$ pb, observed numbers of data events and measured $\sigma_{t\bar{t}}$ at top mass of 170 GeV/c^2. Quoted uncertainties include both statistical and systematic uncertainties, added in quadrature.

Channel	Luminosity (pb^{-1})	W + jets	Z + jets	Multijet	Other bkg	$t\bar{t}$	Total	Observed	$\sigma_{t\bar{t}}$ (pb)
e + jets (3 jets, 1b tag)	1038	$53.4^{+6.0}_{-6.0}$	$6.0^{+1.2}_{-1.2}$	$31.5^{+3.5}_{-3.5}$	$11.4^{+1.5}_{-1.4}$	$81.7^{+6.4}_{-6.7}$	$184.0^{+9.0}_{-9.2}$	183	$8.06^{+1.89}_{-1.71}$
μ + jets (3 jets, 1b tag)	996	$59.2^{+5.5}_{-5.6}$	$6.5^{+1.3}_{-1.3}$	$9.7^{+2.8}_{-2.8}$	$9.5^{+1.2}_{-1.2}$	$59.0^{+5.7}_{-5.6}$	$143.9^{+8.1}_{-8.1}$	133	$6.43^{+2.22}_{-2.01}$
e + jets (3 jets, $\geq 2b$ tags)	1038	$5.0^{+0.8}_{-0.8}$	$0.6^{+0.2}_{-0.2}$	$2.7^{+0.3}_{-0.3}$	$2.4^{+0.4}_{-0.4}$	$30.7^{+3.9}_{-3.9}$	$41.5^{+4.7}_{-4.6}$	40	$7.78^{+2.41}_{-2.01}$
μ + jets (3 jets, $\geq 2b$ tags)	996	$5.8^{+0.9}_{-0.9}$	$0.7^{+0.2}_{-0.2}$	$1.0^{+0.3}_{-0.3}$	$2.1^{+0.3}_{-0.3}$	$23.8^{+3.4}_{-3.2}$	$33.5^{+4.1}_{-3.9}$	31	$7.29^{+2.73}_{-2.25}$
e + jets (≥ 4 jets, 1b tag)	1038	$8.5^{+2.7}_{-2.7}$	$2.2^{+0.5}_{-0.5}$	$7.9^{+1.0}_{-1.0}$	$3.0^{+0.5}_{-0.5}$	$81.6^{+8.7}_{-9.1}$	$103.3^{+7.3}_{-7.6}$	113	$9.38^{+1.82}_{-1.52}$
μ + jets (≥ 4 jets, 1b tag)	996	$13.6^{+2.6}_{-2.7}$	$2.5^{+0.7}_{-0.6}$	$0.0^{+0.0}_{-0.0}$	$2.4^{+0.4}_{-0.4}$	$65.9^{+6.9}_{-7.2}$	$84.3^{+5.9}_{-6.3}$	99	$10.44^{+2.11}_{-1.76}$
e + jets (≥ 4 jets, $\geq 2b$ tags)	1038	$1.0^{+0.3}_{-0.3}$	$0.2^{+0.1}_{-0.1}$	$1.1^{+0.1}_{-0.1}$	$0.9^{+0.2}_{-0.2}$	$41.7^{+6.0}_{-6.0}$	$44.9^{+6.0}_{-6.0}$	30	$5.12^{+1.59}_{-1.28}$
μ + jets (≥ 4 jets, $\geq 2b$ tags)	996	$1.5^{+0.4}_{-0.4}$	$0.3^{+0.1}_{-0.1}$	$0.0^{+0.0}_{-0.0}$	$0.7^{+0.1}_{-0.1}$	$35.6^{+5.0}_{-5.1}$	$38.2^{+5.1}_{-5.2}$	34	$7.60^{+2.11}_{-1.70}$
ee	1074		$2.3^{+0.5}_{-0.5}$	$0.6^{+0.4}_{-0.4}$	$0.5^{+0.1}_{-0.1}$	$11.6^{+1.2}_{-1.2}$	$15.0^{+1.5}_{-1.5}$	17	$9.61^{+3.47}_{-2.84}$
$e\mu$ (1 jet)	1070		$5.5^{+0.7}_{-0.8}$	$0.9^{+0.3}_{-0.2}$	$3.1^{+0.7}_{-0.7}$	$8.9^{+1.4}_{-1.4}$	$18.4^{+1.9}_{-1.9}$	21	$10.61^{+5.33}_{-4.23}$
$e\mu$ (≥ 2 jets)	1070		$5.4^{+0.9}_{-1.0}$	$2.6^{+0.6}_{-0.5}$	$1.4^{+0.4}_{-0.4}$	$36.4^{+3.6}_{-3.6}$	$45.8^{+4.5}_{-4.5}$	39	$6.66^{+1.81}_{-1.52}$
$\mu\mu$	1009		$5.6^{+1.1}_{-1.2}$	$0.2^{+0.2}_{-0.2}$	$0.6^{+0.1}_{-0.1}$	$9.1^{+1.0}_{-1.0}$	$15.4^{+1.8}_{-1.9}$	12	$5.08^{+3.82}_{-3.06}$
τe ($\geq 1b$ tag)	1038	$0.6^{+0.0}_{-0.1}$	$0.6^{+0.1}_{-0.1}$	$3.0^{+1.7}_{-1.7}$	$0.2^{+0.1}_{-0.1}$	$10.7^{+1.3}_{-1.3}$	$15.0^{+2.2}_{-2.2}$	16	$8.94^{+4.03}_{-3.32}$
$\tau\mu$ ($\geq 1b$ tag)	996	$0.8^{+0.1}_{-0.2}$	$1.2^{+0.3}_{-0.3}$	$8.0^{+2.8}_{-2.8}$	$0.2^{+0.0}_{-0.0}$	$12.6^{+1.4}_{-1.4}$	$22.7^{+3.2}_{-3.2}$	20	$6.40^{+3.88}_{-3.43}$

lepton acceptance ($|\eta| < 1.1$) compared to the μ + jets channel ($|\eta| < 2.0$). In addition, the wider rapidity distribution of the W + jets events compared to $t\bar{t}$ events increases the W + jets background contribution in the μ + jets channel.

To calculate the combined cross section, we define a joint likelihood function as the product of Poisson probabilities for the 14 disjoint subsamples, as listed in Table I. Fourteen additional Poisson terms constrain the multijet background in the ℓ + jets and $\tau\ell$ channels. In particular, for the τe and $\tau\mu$ channels, the multijet background is determined by counting events with an electron or muon and associated τ of the same electric charge, introducing a corresponding Poisson term per channel. In the ℓ + jets channel, we estimate the multijet background separately for each of the eight subchannels by using corresponding control data samples [15]. Four additional terms arise from applying this same method in evaluating the multijet background before b tagging.

Each systematic uncertainty is included in the likelihood function through one free ''nuisance'' parameter [15]. Each of these parameters is represented by a Gaussian probability density function with zero mean and a standard deviation of one; all are allowed to float in the maximization of the likelihood function, thereby changing the central value of the measured $\sigma_{t\bar{t}}$. Correlations are taken into account by using the same nuisance parameter for a common source of systematic uncertainty in different channels scaled by the corresponding standard deviation (SD) of each individual channel. Thus, the likelihood function to be maximized is represented by the product

$$\mathcal{L} = \prod_{i=1}^{14} \mathcal{P}(n_i, m_i) \times \prod_{j=1}^{14} \mathcal{P}(n_j, m_j) \times \prod_{k=1}^{K} \mathrm{SD}_{ik} \times \mathcal{G}(\nu_k; 0, 1), \quad (1)$$

where $\mathcal{P}(n, m)$ is the Poisson probability to observe n events given the expectation of m events. The predicted number of events in each channel is the sum of the predicted background and expected $t\bar{t}$ events, which depends on $\sigma_{t\bar{t}}$. In the product, i runs over the subsamples and j runs over the multijet background subsamples. The Gaussian distributions $\mathrm{SD}_{ik} \times \mathcal{G}(\nu_k; 0, 1)$ describe the systematic uncertainties, K is the total number of independent sources of systematic uncertainty, ν_k are the individual nuisance parameters, and SD_{ik} is 1 standard deviation for the source of uncertainty k in subsample i.

Systematic uncertainties on the measured $\sigma_{t\bar{t}}$ are evaluated from sources that include electron and muon identification; τ and jet identification and energy calibration; b-jet identification; modeling of triggers, signal, and background; and integrated luminosity. All these uncertainties are treated as fully correlated among channels and between signal and background. Systematic uncertainties arising from limited statistics of data or Monte Carlo samples used in estimating signal or backgrounds are considered to be uncorrelated. A detailed discussion on systematic uncertainties can be found in Refs. [7,8]. Table II shows a breakdown of uncertainties on the combined cross section. We evaluate the effect from each source by setting all uncertainties to zero except the one in question and redoing the likelihood maximization with respect to only the corresponding nuisance parameter. Since the method allows each uncertainty to change the central value, the total uncertainty on $\sigma_{t\bar{t}}$ differs slightly from the quadratic sum of the statistical and individual systematic uncertainties. The total systematic uncertainty on $\sigma_{t\bar{t}}$ exceeds the statistical contribution. The luminosity uncertainty of 6.1% which enters into the estimation of the majority of the backgrounds and the luminosity measurement of the selected samples is the dominant source of systematic uncertainty.

TABLE II. Summary of uncertainties on the combined $\sigma_{t\bar{t}}$.

Source	$\Delta\sigma_{t\bar{t}}$ (pb)	
Statistical	+0.47	−0.46
Lepton identification	+0.15	−0.14
Tau identification	+0.02	−0.02
Jet identification	+0.11	−0.11
Jet energy scale	+0.19	−0.16
Tau energy scale	+0.02	−0.02
Trigger modeling	+0.11	−0.07
b-jet identification	+0.34	−0.32
Signal modeling	+0.17	−0.15
Background estimation	+0.14	−0.14
Multijet background	+0.12	−0.12
Luminosity	+0.56	−0.48
Other	+0.15	−0.14
Total systematic uncertainty	+0.78	−0.69

Table III summarizes the individual $\sigma_{t\bar{t}}$ measurements for the individual channels, as well as some of their combinations. Within uncertainties, all measurements are consistent with each other. The combined cross section for ℓ + jets, $\ell\ell$, and $\tau\ell$ final states for a top quark mass of 170 GeV/c^2 is evaluated to be

$$\sigma_{t\bar{t}} = 8.18^{+0.98}_{-0.87}\ \text{pb}, \tag{2}$$

in agreement with theoretical predictions [1–4]. The uncertainty is comparable to the one on the cross section combination from different methods in the ℓ + jets channel performed by D0 [8]. The observed number of events in the different channels is compared to the sum of the background and combined $t\bar{t}$ signal in Fig. 1(a).

We compute ratios R_σ of measured cross sections, $R_\sigma^{\ell\ell/\ell j} = \sigma_{t\bar{t}}^{\ell\ell}/\sigma_{t\bar{t}}^{\ell j}$ and $R_\sigma^{\tau\ell/\ell\ell\text{-}\ell j} = \sigma_{t\bar{t}}^{\tau\ell}/\sigma_{t\bar{t}}^{\ell j\&\ell\ell}$, by generating pseudodata sets in the numerator and denominator in order to take into account the correlation between systematic uncertainties. $\sigma_{t\bar{t}}^{\text{channel}}$ represent the measured cross sections in the corresponding channel. The pseudodata sets are created by varying the number of signal and background events around the expected number according to Poisson probabilities. All independent sources of systematic uncertainties are varied within a Gaussian distribution. Although the individual channels considered are exclusive, each channel can receive signal contributions from different $t\bar{t}$ decay modes. We calculate the contribution from dilepton events to the ℓ + jets final state as well as the contribution from dilepton and ℓ + jets events to the $\tau\ell$ final states using the corresponding observed cross sections in the individual channels when generating pseudodata sets. For each pseudodata set, we perform the maximization of Eq. (1) separately in the numerator and denominator, and divide the results. The central value is obtained from the mode of the distribution of R_σ, and the uncertainties are derived from the interval containing 68% of the pseudoexperiments. From these pseudoexperiments we obtain $R_\sigma^{\ell\ell/\ell j} = 0.86^{+0.19}_{-0.17}$ and $R_\sigma^{\tau\ell/\ell\ell\text{-}\ell j} = 0.97^{+0.32}_{-0.29}$, which is consistent with the SM expectation of $R_\sigma = 1$.

TABLE III. Summary of measured $\sigma_{t\bar{t}}$ in different channels for $m_t = 170$ GeV/c^2.

Channel	$\sigma_{t\bar{t}}$ (pb)
ℓ + jets	$8.46^{+1.09}_{-0.97}$
$\ell\ell$ [7]	$7.46^{+1.60}_{-1.37}$
ℓ + jets and $\ell\ell$	$8.18^{+0.99}_{-0.87}$
$\tau\ell$ [7]	$7.77^{+2.90}_{-2.47}$
ℓ + jets, $\ell\ell$, and $\tau\ell$	$8.18^{+0.98}_{-0.87}$

Extensions of the SM, based on supersymmetry or grand unification [5], require the existence of additional Higgs multiplets beyond the Higgs doublet of the SM. Some of these models, such as the two Higgs-doublet model or the minimal supersymmetric standard model, foresee the existence of physical degrees of freedom which can be associated with a charged scalar particle, the charged Higgs boson. If this charged Higgs boson is lighter than the top quark, it will appear in the top quark decays. We use the ratios to extract upper limits on the branching ratio $B \equiv B(t \to H^+ b)$. In particular, a charged Higgs boson decaying into a tau and a neutrino ($B(H^+ \to \tau\nu) = 1$) results in more events in the $\tau\ell$ channel, while fewer events appear in the $\ell\ell$ and ℓ + jets final states compared to the SM prediction. In case of a leptophobic ($B(H^+ \to c\bar{s}) = 1$) model, the number of dilepton events decreases faster than the number of ℓ + jets events for increasing $B(t \to H^+ b)$. We therefore use $R_\sigma^{\ell\ell/\ell j}$ to set limits on the leptophobic model, while $R_\sigma^{\tau\ell/\ell\ell\text{-}\ell j}$ is used to search for decays in which the charged Higgs bosons are assumed to decay exclusively to taus.

To extract the limits, we generate pseudodata sets assuming different branching fractions $B(t \to H^+ b)$. The signal for a charged Higgs boson is simulated using the PYTHIA Monte Carlo event generator [13], and includes decays of $t\bar{t} \to W^+ b H^- \bar{b}$ and its charge conjugate (WH) and $t\bar{t} \to H^+ b H^- \bar{b}$ (HH). For a given branching fraction B, we calculate the expected number of $t\bar{t}$ events per final state,

$$N_{t\bar{t}} = [(1-B)^2 \cdot \epsilon_{WW} + 2B(1-B) \cdot \epsilon_{WH} + B^2 \cdot \epsilon_{HH}]\sigma_{t\bar{t}} L, \tag{3}$$

where ϵ are the selection efficiencies for the different decays (WW refers to $t\bar{t} \to W^+ b W^- \bar{b}$) and L is the integrated luminosity. We add $N_{t\bar{t}}$ to the expected background and treat the sum as a new number of expected events in each channel. We then perform the likelihood maximization to extract $\sigma_{t\bar{t}}$ from these pseudodata as if they contained only SM $t\bar{t}$ production. This provides distributions for the ratios of cross sections for each generated B, which are compared to the observed ratio. We set limits on B by

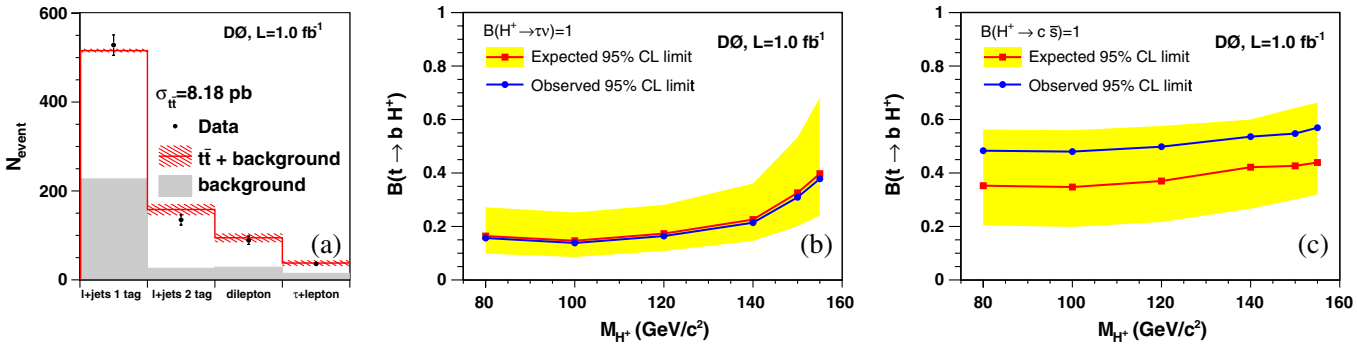

FIG. 1 (color online). (a) Expected and observed numbers of events versus channel used in measuring the combined $\sigma_{t\bar{t}}$. The dashed band around the prediction indicates the total uncertainty. Upper limits on $B(t \to H^+ b)$ for (b) tauonic and (c) leptophobic H^+ decays. The yellow band shows the ± 1 standard deviation band around the expected limit.

using the frequentist approach of Feldman and Cousins [16].

The observed and expected (i.e., for $R_\sigma = 1$) limits for the tauonic and the leptophobic charged Higgs boson models are shown in Figs. 1(b) and 1(c), respectively. In the tauonic model the upper 95% C.L. limits on B range from 15% to 40% for 80 GeV$/c^2 \leq M_{H^+} \leq$ 155 GeV$/c^2$, improving the limits given in [17]. For the leptophobic charged Higgs boson model, which is investigated here for the first time, the upper limit on the B range is between 48% and 57% for the same mass range. Although indirect bounds as those from the measured rate of $b \to s\gamma$ [18] appear stronger than the results from the direct search presented here, they can be invalidated by the presence of new physics contributions.

The interpretation of the direct measurement of the top quark mass [6] has become a subject of intense discussion in terms of its renormalization scheme [19]. The extraction of this parameter from the measured cross section provides complementary information, with different sensitivity to theoretical and experimental uncertainties, relative to direct methods that rely on kinematic details of the top quark reconstruction. Simulated samples of $t\bar{t}$ events generated at different values of the top quark mass are used to estimate the signal acceptance. The resulting measurements of $\sigma_{t\bar{t}}$ are fitted as a function of m_t [2]:

$$\sigma_{t\bar{t}}(m_t) = \frac{1}{m_t^4}[a + b(m_t - m_0) + c(m_t - m_0)^2 + d(m_t - m_0)^3] \quad (4)$$

where $\sigma_{t\bar{t}}$ and m_t are in pb and GeV$/c^2$, respectively, and $m_0 = 170$ GeV$/c^2$ [20]. The dependence on the top quark mass is due to the mass dependence of the selection efficiencies.

We compare this parametrization to a prediction in pure next-to-leading-order (NLO) QCD [1], to a calculation including NLO QCD and all higher-order soft-gluon resummations in next-to-leading logarithms (NLL) [2], to an approximation to the next-to-next-to-leading-order (NNLO) QCD cross section that includes all next-to-next-to-leading logarithms relevant in NNLO QCD [3], and to a calculation that employs full kinematics in the double differential cross section beyond NLL using the soft anomalous dimension matrix to calculate the soft-gluon contributions at NNLO [4]. Figure 2 shows the experimental and the theoretical [1–3] $t\bar{t}$ cross sections as a function of the top quark mass.

Following the method of Refs. [7,8], we extract the most probable top quark mass values and the 68% C.L. band. Since the theoretical predictions are performed in the pole mass scheme, this defines the extracted parameter here. The results are given in Table IV. All values are in good agreement with the current world average of 171.2 ± 2.1 GeV$/c^2$ [6].

In summary, we have combined the $t\bar{t}$ cross section measurements in ℓ + jets, $\ell\ell$, and $\tau\ell$ channels to measure $\sigma_{t\bar{t}} = 8.18^{+0.98}_{-0.87}$ pb for a top quark mass of 170 GeV$/c^2$. For the first time, we have also calculated ratios of cross

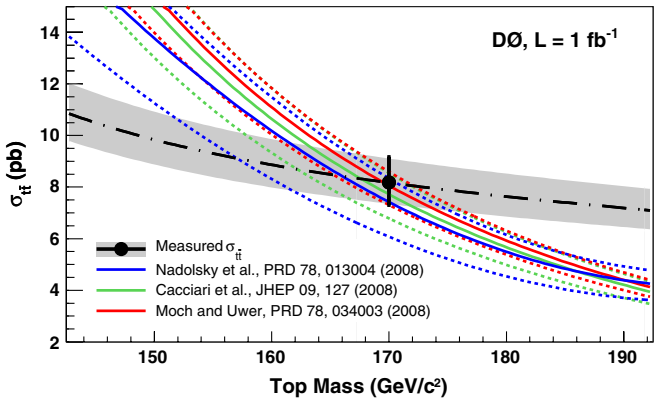

FIG. 2 (color online). Experimental and theoretical [1–3] $\sigma_{t\bar{t}}$ as a function of m_t. The colored dashed lines represent the theoretical uncertainties due to the choice of the PDF and the renormalization and factorization scales. The point shows the measured combined $\sigma_{t\bar{t}}$, the black dot-dashed line shows the fit with Eq. (4), and the gray band shows the corresponding total experimental uncertainty.

TABLE IV. Top quark mass with 68% C.L. region for different theoretical predictions of $\sigma_{t\bar{t}}$. Combined experimental and theoretical uncertainties are shown.

Theoretical prediction	m_t (GeV/c^2)
NLO [1]	$165.5^{+6.1}_{-5.9}$
NLO + NLL [2]	$167.5^{+5.8}_{-5.6}$
Approximate NNLO [3]	$169.1^{+5.9}_{-5.2}$
Approximate NNLO [4]	$168.2^{+5.9}_{-5.4}$

sections and interpreted them in terms of limits on nonstandard model top quark decays into a charged Higgs boson. All results are in good agreement with the SM expectations. Finally, using different theoretical predictions given in the pole mass scheme, we have extracted the top quark mass from the combined $\sigma_{t\bar{t}}$ and have found the result to be consistent with the world average top quark mass [6] from direct measurements.

We thank the staffs at Fermilab and the collaborating institutions, and acknowledge support from the DOE and NSF (USA); CEA and CNRS/IN2P3 (France); FASI, Rosatom, and RFBR (Russia); CNPq, FAPERJ, FAPESP, and FUNDUNESP (Brazil); DAE and DST (India); Colciencias (Colombia); CONACyT (Mexico); KRF and KOSEF (Korea); CONICET and UBACyT (Argentina); FOM (the Netherlands); STFC and the Royal Society (United Kingdom); MSMT and GACR (Czech Republic); CRC Program, CFI, NSERC, and WestGrid Project (Canada); BMBF and DFG (Germany); SFI (Ireland); the Swedish Research Council (Sweden); CAS and CNSF (China); and the Alexander von Humboldt Foundation (Germany).

[1] P. M. Nadolsky *et al.*, Phys. Rev. D **78**, 013004 (2008); W. Beenakker, H. Kuijf, W. L. vanNeerven, and J. Smith, Phys. Rev. D **40**, 54 (1989).
[2] M. Cacciari *et al.*, J. High Energy Phys. 09 (2008) 127; M. Cacciari (private communications).
[3] S. Moch and P. Uwer, Phys. Rev. D **78**, 034003 (2008); (private communications).
[4] N. Kidonakis and R. Vogt, Phys. Rev. D **78**, 074005 (2008); N. Kidonakis (private communications).
[5] J. Guasch, R. A. Jimenez, and J. Sola, Phys. Lett. B **360**, 47 (1995).
[6] C. Amsler *et al.* (Particle Data Group), Phys. Lett. B **667**, 1 (2008).
[7] V. M. Abazov *et al.* (D0 Collaboration), Phys. Lett. B **679**, 177 (2009).
[8] V. M. Abazov *et al.* (D0 Collaboration), Phys. Rev. Lett. **100**, 192004 (2008).
[9] V. M. Abazov *et al.* (D0 Collaboration), Phys. Rev. D **76**, 092007 (2007).
[10] V. M. Abazov *et al.* (D0 Collaboration), Phys. Rev. D **76**, 052006 (2007).
[11] T. Scanlon, Ph.D. thesis, Imperial College, London [Institution Report No. FERMILAB-THESIS-2006-43, 2006].
[12] M. L. Mangano *et al.*, J. High Energy Phys. 07 (2003) 001.
[13] T. Sjöstrand *et al.*, Comput. Phys. Commun. **135**, 238 (2001).
[14] E. E. Boos *et al.*, Phys. At. Nucl. **69**, 1317 (2006).
[15] V. M. Abazov *et al.* (D0 Collaboration), Phys. Rev. D **74**, 112004 (2006).
[16] G. J. Feldman and R. D. Cousins, Phys. Rev. D **57**, 3873 (1998).
[17] A. Abulencia *et al.* (CDF Collaboration), Phys. Rev. Lett. **96**, 042003 (2006).
[18] M. Misiak *et al.*, Phys. Rev. Lett. **98**, 022002 (2007).
[19] A. H. Hoang and I. W. Stewart, Nucl. Phys. B, Proc. Suppl. **185**, 220 (2008).
[20] We obtain $a = 6.823\,50 \times 10^9$, $b = 1.104\,80 \times 10^8$, $c = 8.805\,52 \times 10^5$, and $d = -1.767 \times 10^3$ for Eq. (4).